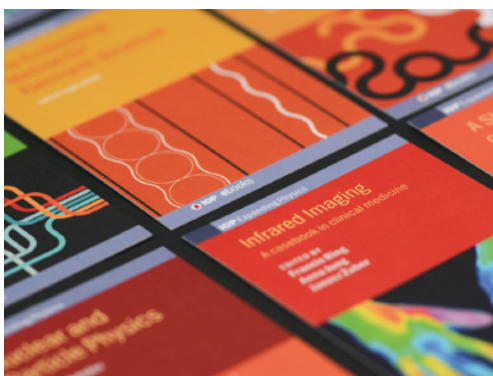


PAPER

# Competition between pinning produced by extrinsic random point disorder and superconducting thermal fluctuations in oxygen-deficient $\text{GdBa}_2\text{Cu}_3\text{O}_x$ coated conductors

To cite this article: N Haberkorn *et al* 2019 *Supercond. Sci. Technol.* **32** 125015

View the [article online](#) for updates and enhancements.



**IOP | ebooks™**

Bringing together innovative digital publishing with leading authors from the global scientific community.

Start exploring the collection—download the first chapter of every title for free.

# Competition between pinning produced by extrinsic random point disorder and superconducting thermal fluctuations in oxygen-deficient $\text{GdBa}_2\text{Cu}_3\text{O}_x$ coated conductors

N Haberkorn<sup>1,2</sup> , J Guimpel<sup>1,2</sup>, S Suárez<sup>1,2</sup>, Jae-Hun Lee<sup>3</sup>, Hunju Lee<sup>3</sup> and S H Moon<sup>3</sup>

<sup>1</sup> Comisión Nacional de Energía Atómica and Consejo Nacional de Investigaciones Científicas y Técnicas, Centro Atómico Bariloche, Av. Bustillo 9500, 8400 San Carlos de Bariloche, Argentina

<sup>2</sup> Instituto Balseiro, Universidad Nacional de Cuyo y Comisión Nacional de Energía Atómica, Av. Bustillo 9500, 8400 San Carlos de Bariloche, Argentina

<sup>3</sup> SuNAM Co. Ltd, Ansung, Gyeonggi-Do 430-817, Republic of Korea

E-mail: [nhaberk@cab.cnea.gov.ar](mailto:nhaberk@cab.cnea.gov.ar)

Received 4 August 2019, revised 16 October 2019

Accepted for publication 25 October 2019

Published 13 November 2019



CrossMark

## Abstract

We report on the influence of random point defects introduced by 3 MeV proton irradiation on the vortex dynamics of 1.3  $\mu\text{m}$  thick  $\text{GdBa}_2\text{Cu}_3\text{O}_x$  coated conductors. Thin films with different oxygen stoichiometry ( $6.7 < x < 7$ ) were irradiated with 3 MeV proton (p) using a fluence of  $2 \times 10^{16} \text{ p cm}^{-2}$ . We find a direct correlation between the changes in  $T_c$  produced by oxygen content and damage by irradiation on the resulting vortex dynamics in the films. The analysis of the critical current densities  $J_c$  at low temperatures indicates that although irradiation produces smooth magnetic field dependences, the self-field values decrease systematically as  $T_c$  reduces. Moreover, the analysis of the relaxation of the persistent currents shows that the characteristic glassy exponent  $\mu$  systematically decreases from 1.7 to 0.66 as  $T_c$  decreases from 93 to 55 K.

Keywords: vortex dynamics, coated conductors, oxygen stoichiometry, proton irradiation

(Some figures may appear in colour only in the online journal)

## 1. Introduction

Understanding the interplay between thermal fluctuations and vortex pinning represents an essential task to improve critical current densities  $J_c$  in high-temperature superconductors (HTS) [1]. Immobilizing vortices, usually by pinning onto material defects, is of high technological relevance. Depending on the temperature and range of applications, the pinning landscape is optimizing by combining defects of different size, shape, and density. Due to the complexity of introducing diverse types of defects in a single step during the fabrication process, the irradiation appears as a powerful tool to enhance the magnetic field dependences of  $J_c$  at low temperatures [2–6]. Depending on the

mass and energy of the ions and the properties of the superconducting material, irradiation enables the creation of defects such as points, clusters, or tracks [1, 7]. The maximum enhancement in  $J_c$  is a compromise between improving vortex pinning and diminishing the suppression in the superconductor properties. Indeed, the superconducting critical temperature  $T_c$  in HTS usually decreases as the damage produced by irradiation increases [2, 8]. Moreover, while the  $J_c$  values at high magnetic fields improve, its values at self-field ( $J_c^{\text{sf}}$ ) reduce [2, 8, 9]. Additionally, the disorder at the nanoscale produced by the irradiation induces a counterintuitive increment in the relaxation of the persistent currents,  $S = -\delta \ln J / \delta \ln t$  (with  $t$  the time), at intermediate and high temperatures [2, 8, 9].

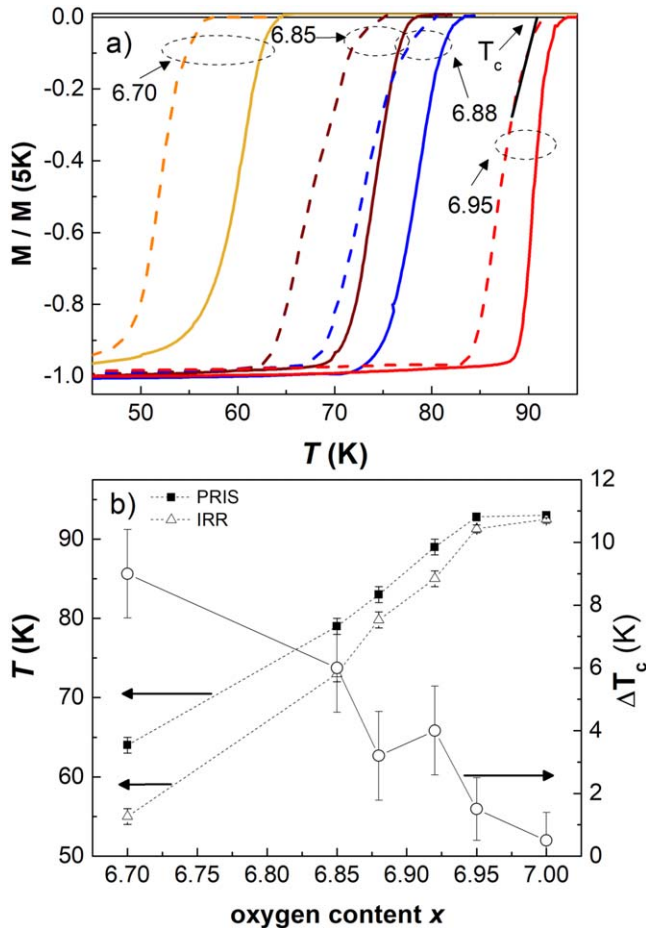


**Figure 1.** (a) Temperature dependence of the normalized magnetization ( $M/M(5\text{ K})$ ) temperature for  $\text{GdBa}_2\text{Cu}_3\text{O}_x$  films before (PRIS, solid line) and after (IRR, dashed line) proton irradiation. (b) Summary of the dependence of the superconducting critical temperature ( $T_c$ ) with oxygen content for  $\text{GdBa}_2\text{Cu}_3\text{O}_x$  films before and after irradiation with 3 MeV protons (left). Difference in the superconducting critical temperature ( $\Delta T_c$ ) as function of oxygen content for  $\text{GdBa}_2\text{Cu}_3\text{O}_x$  tapes before and after irradiation (right). The measurement were performed with  $\mu_0 H = 0.5\text{ mT}$  with  $\mathbf{H}/c$ -axis after zero field cooling.

The reduction in  $J_c^{sf}$  for irradiated coated conductors may be related to the suppression of the superfluid density due to disorder at the nanoscale [10–12]. The increment in vortex fluctuations, due to changes in the penetration depth ( $\lambda$ ), also is evidenced as a reduction of the  $J_c$  values in the overall range of fields at high temperatures [8]. The variations in the relaxation of the persistent currents at middle and high temperatures have been ascribed to changes in the vortex bundle size due to the addition of random disorder [9]. On the other hand, oxygen-deficient  $\text{GdBa}_2\text{Cu}_3\text{O}_x$  films display a direct correlation between the reduction in  $T_c$ ,  $J_c^{sf}$  and the increment in the  $S$  values [13]. Although  $T_c$  is reduced with both irradiation and changes in the oxygen stoichiometry, the latter produces larger suppression of the  $J_c^{sf}$  values. This effect can be associated with changes in the upper critical field anisotropy  $\gamma$  [14, 15]. It is known that for a constant oxygen stoichiometry,  $\gamma$  increases as  $T_c$  reduces. No change on  $\gamma$  with suppressing  $T_c$  has been reported for irradiation. Due to this

difference, it is useful to analyze the influence of the irradiation on the vortex dynamics of oxygen-deficient  $\text{GdBa}_2\text{Cu}_3\text{O}_x$  films. In that case, the properties will be given by a competition between the improvement in the pinning due to new point defects and the increment in the vortex fluctuations due to the reduction in  $T_c$ .

Here, we report on the influence of adding random point disorder on the vortex dynamics of oxygen-deficient  $1.3\text{ }\mu\text{m}$  thick  $\text{GdBa}_2\text{Cu}_3\text{O}_x$  (GBCO) tapes grown by co-evaporation [16]. Films with different oxygen stoichiometry ( $6.7 < x < 7$ ) were irradiated with 3 MeV protons to a fluence of  $2 \times 10^{16}\text{ p cm}^{-2}$ . The  $x$  range was selected avoiding the dimensional crossover from a 3D to a quasi-2D vortex system ( $x \approx 6.5$ ) [15]. The objective of the present manuscript is to find a correlation between the vortex dynamics and  $J_c$  values in thin films in which  $T_c$  is suppressed by changes in the oxygen content and by disorder introduced by irradiation [9, 13]. The pinning landscape in unirradiated films is produced mainly by  $\text{Gd}_2\text{O}_3$  inclusions with a typical size of  $\approx 50\text{ nm}$  [17]. We study the persistent current density  $J_c$  and its decay with time from magnetic hysteresis measurements and relaxation studies, respectively. The results for the irradiated films are compared and contrasted with our previous results as a function of oxygen stoichiometry [13]. We observe that the irradiation systematically reduces  $T_c$ , with a more significant effect for smaller oxygen content. Although the irradiation produces smooth  $J_c(H)$  dependences,  $J_c^{sf}$  systematically decreases as  $T_c$  reduces. Moreover, the analysis of the vortex dynamics shows similar changes in flux creep rates at intermediate and high temperatures when  $T_c$  reduces by either changing the oxygen stoichiometry or by adding disorder with irradiation.

## 2. Material and methods

The GBCO tape was grown by the co-evaporation technique on  $\text{LaMnO}_3$  (LMO)-buffered IBAD-MgO templates [18]. The oxygen content  $x$  of the tapes was adjusted to the desired value by using the iso-stoichiometric anneal method [19]. The sample is heated in an  $\text{O}_2$  pressure of 11.5 Torr at an annealing temperature  $T_{ann}(x)$  which is determined by the desired stoichiometry ( $490\text{ }^\circ\text{C}$  for  $x = 6.7$  and  $410\text{ }^\circ\text{C}$  for  $x = 6.95$ ). After 2 h the film was slowly cooled down at a  $1\text{ }^\circ\text{C min}^{-1}$  rate, while the  $\text{O}_2$  pressure was continually adjusted to follow the corresponding constant  $x$  line in the  $\text{O}_2$  pressure versus  $T$  phase diagram.

Films with different oxygen stoichiometry were irradiated with 3 MeV proton to a fluence of  $2 \times 10^{16}\text{ p cm}^{-2}$ . This value corresponds to the optimal value to enhance pinning in pristine YBCO single crystals [20] and GBCO tapes [8]. The irradiation was performed at room temperature on pieces with typical area  $1.2 \times 1.2\text{ mm}^2$  using ion beam currents of  $\approx 10\text{ nA}$ . In all cases, the ion beam impacted perpendicular to the surface of the samples. To guarantee good thermal contact, the samples were fixed to the holder with silver paint. The irradiations were performed with the ion beam positioned at the center of the sample. The size of the

beam has  $\approx 1.5$  mm. 3 MeV protons are known to produce from one to a few tens of atom displacements, producing mainly random point defects and also some nanoclusters of a few nanometers in size [21].

Magnetization ( $M$ ) measurements were performed in a superconducting quantum interference device (SQUID) magnetometer with the applied magnetic field ( $H$ ) parallel to the  $c$ -axis ( $\mathbf{H} \parallel c$ ) (perpendicular to the surface). The  $T_c$  were determined from  $M(T)$  at  $\mu_0 H = 0.5$  mT after zero field cooling. The  $J_c$  values were calculated from the magnetization data using the appropriate geometrical factor in the Bean Model [22]. For  $\mathbf{H} \parallel c$ ,  $J_c = \frac{20\Delta M}{w(1-w/3l)}$ , where  $\Delta M$  is the difference in magnetization between the top and bottom branches of the hysteresis loop,  $l$  and  $w$  are the length and width of the film ( $l > w$ ), respectively. The  $M$  versus time measurements were recorded for more than 1 h. The initial time was adjusted considering the best correlation factor in the log–log linear fit of the  $J_c(t)$  dependence. To ensure a critical state, the initial state for each measurement was generated using a field variation  $\Delta H \sim 4H^*$ , where  $H^*$  is the field for full-flux penetration [23].

### 3. Results and discussion

Figure 1(a) shows typical curves of reduced magnetization ( $M/M(5\text{ K})$ ) for GBCO films with different oxygen content. The results indicate that  $T_c$  decreases with  $x$  [13]. Moreover,  $T_c$  systematically drops for proton-irradiated films (see table 1). Figure 1(b) (left axis) displays a summary of the obtained values as a function of  $x$ . As is evident from this plot, the suppression of  $T_c$  produced by irradiation is larger as  $x$  is reduced (see right axis figure 1(b)).

Figure 2(a) shows typical curves of the magnetic field dependence of  $J_c$  for  $\text{GdBa}_2\text{Cu}_3\text{O}_x$  films before (full symbol) and after (open symbol) irradiation at  $T = 5$  K. The data can be analyzed considering  $J_c^{sf}$  and the magnetic field dependence of  $J_c$ . The latter can be parameterized considering a power-law dependence with  $J_c \propto H^{-\alpha}$ . The exponent  $\alpha$  is usually related to the type of pinning centers being  $\approx 0.5$ – $0.62$  for pinning produced by random nanoparticles [24]. Moreover, tapes growth on IBAD-MgO templates usually display correlated pinning due to island boundaries [18, 25]. The results indicate that  $J_c^{sf}$  decreases with the changes in  $x$  [13] and with irradiation [8]. Figure 2(b) displays a summary of  $J_c^{sf}$  as function of  $T_c$ . Data for fully oxygenated films are also included [8]. For unirradiated and irradiated films, there is a clear correlation between  $T_c$  and  $J_c^{sf}$ . Figure 2(c) shows the evolution of  $\alpha$  with  $T_c$  for the same films before and after irradiation. As is evident, for pristine films with  $x = 6.92, 6.95$  and  $7$ ,  $\alpha$  remains  $\approx 0.63$  [13]. For  $x = 6.85$  and  $6.88$ ,  $\alpha$  increases to  $\approx 0.66$ . Finally,  $\alpha \approx 0.72$  for  $x = 6.7$ . For irradiated films,  $\alpha$  decreases to  $0.49$  for  $x = 7$  and increases monotonically to  $0.6$  for  $x = 6.85$ . No power-law dependence is observed for  $x = 6.7$  after irradiation. The change in  $\alpha$  becomes smaller as  $T_c$  reduces, indicating a less effective pinning of

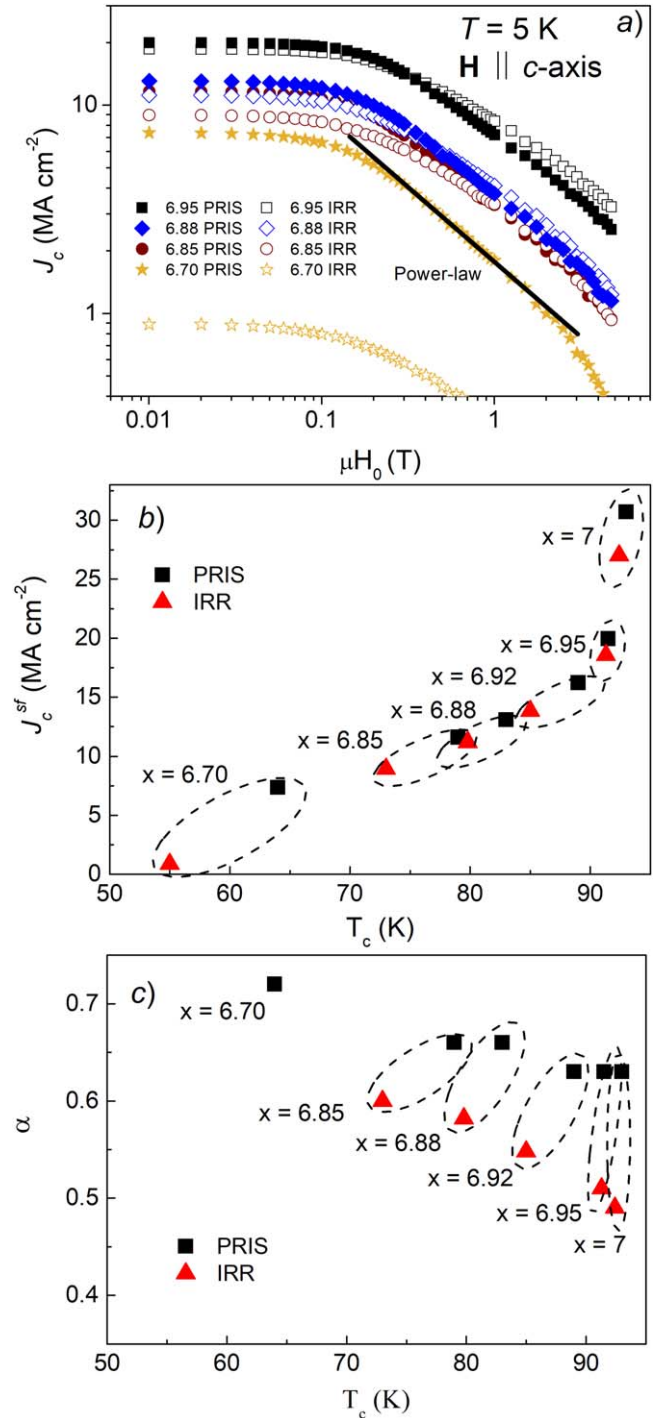


**Figure 2.** (a) Magnetic field dependence of the critical current densities  $J_c$  in  $\text{GdBa}_2\text{Cu}_3\text{O}_x$  films before (PRIS, full symbol) and after proton irradiation (IRR, open symbol). (b), (c) Self-field critical current density and power law  $\alpha$  ( $J_c \propto H^{-\alpha}$ ) for  $\text{GdBa}_2\text{Cu}_3\text{O}_x$  films before (PRIS) and after (IRR) proton irradiation, respectively. Data of [8] and [13] are included.

random disorder and nanoclusters as  $\gamma$  increases. The  $J_c^{sf}$  (5 K) and  $\alpha$  (5 K) are summarized in table 1.

To analyze in detail the correlation between  $T_c$  and the resulting vortex dynamics, we performed magnetic relaxation measurements of the persistent critical currents. The collective



**Table 1.** Summary of samples and related superconducting parameters.

Sample	$T_c$ (K)	$J_c^{sf}$ (5 K) ( $\text{MA cm}^{-2}$ )	$\alpha$	$\mu$
$x = 7$ PRIS	93.0	30.7	0.63	1.63
$x = 7$ IRR	92.5	27.0	0.49	1.52
$x = 6.95$ PRIS	92.0	20.0	0.63	1.35
$x = 6.95$ IRR	91.3	18.5	0.51	1.33
$x = 6.92$ PRIS	89.0	16.2	0.63	1.23
$x = 6.92$ IRR	85.0	13.8	0.55	1.2
$x = 6.88$ PRIS	83.0	13.0	0.66	1.12
$x = 6.88$ IRR	79.8	11.2	0.58	1.09
$x = 6.85$ PRIS	79.0	11.6	0.66	1.06
$x = 6.85$ IRR	73.0	9.0	0.60	0.99
$x = 6.70$ PRIS	64.5	7.3	0.72	0.99
$x = 6.70$ IRR	55.0	0.9	—	0.66

creep theory predicts a temperature dependence of the normalized flux creep rates as

$$S = -\frac{d(\ln J)}{d(\ln t)} = \frac{T}{U_0 + \mu T \ln(t/t_0)} = \frac{T}{U_0} \left( \frac{J}{J_c} \right)^\mu, \quad (1)$$

where  $t_0$  is a vortex hopping attempt time,  $U_0$  is the collective pinning barrier at  $T = 0$  in the absence of a driving force, and  $\mu > 0$  is the regime-dependent glassy exponent determined by the bundle size and the vortex lattice elasticity [26]. This equation predicts an Anderson–Kim mechanism with  $S \approx T/U_0$  at low temperatures and a plateau as the temperature increases and  $S$  approaches to the limit  $(\mu \cdot \ln(t/t_0))^{-1}$ . Figure 3(a) shows a comparison of  $S(T)$  for GdBa<sub>2</sub>Cu<sub>3</sub>O<sub>x</sub> films before and after irradiation with  $\mu_0 H = 0.5$  T. The qualitative features of the curves correspond to the generally observed in HTS thin films. An initial slope with  $S \approx T/U_0$  is followed by a maximum at  $\approx 20$ – $30$  K, which is usually attributed to correlated disorder (such as twin boundaries) [27], and to changes in the strong pinning regimes for nanoparticles [28]. At intermediate temperatures appears a plateau with  $(\mu \cdot \ln(t/t_0))^{-1}$  and finally at high temperatures, there is a crossover to fast creep [29]. Based on nucleation of vortex loops model, for random point defects in the three-dimensional case,  $\mu$  is  $1/7$ ,  $3/2$  or  $5/2$ , and  $7/9$  for single vortex, small-bundle and large-bundle creep, respectively [24]. As we have shown in [13], the initial slope and the  $S$  values at the plateau at intermediate temperatures increases as the oxygen content reduces. Moreover, for the same oxygen content, the curves for irradiated samples show an increment in the  $S(T)$  values. For a better comparison of the data, we extract the  $\mu$  exponent that determines the  $S$  values at intermediate temperatures using the Maley analysis [30]. This method considers that the current density decays as  $\frac{dJ}{dt} = -\left(\frac{J_c}{\tau}\right) e^{-\frac{U_{eff}(J)}{T}}$ , and the effective activation energy  $U_{eff}(J)$  is described by  $U_{eff} = -T \left[ \ln \left| \frac{dJ}{dt} \right| - C \right]$  with  $C$ , a constant factor. The analysis requires to consider a thermal factor  $G(T)$ , which results in  $U_{eff}(J, 0) \approx U_{eff}(J, T)/G(T)$  [31]. The thermal factor  $G(T) \leq 1$  contains the temperature dependence of the superconducting parameters. The exponent  $\mu$  in the limit of  $J \ll J_c$  can be estimated as  $\Delta \ln U(J)/\Delta \ln J$  [32]. Figure 3(b) shows the

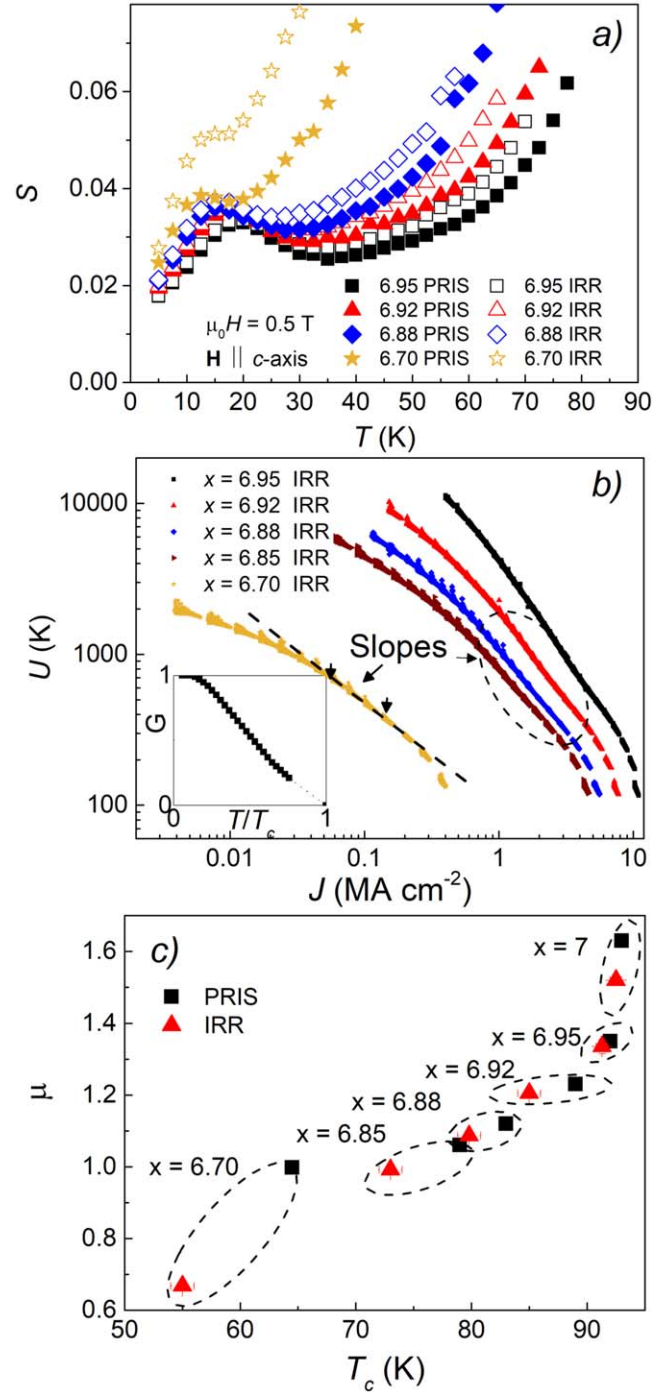


**Figure 3.** (a) Typical temperature dependences of the flux creep rates  $S$  for GBCO films with different oxygen concentration before (PRIS) and after proton (IRR) irradiation. (b) Maley analysis for films with different oxygen concentration after proton irradiation. Inset shows a typical  $G(T)$  function used to maintain the 'piecewise' continuity.

Maley analyzes for GdBa<sub>2</sub>Cu<sub>3</sub>O<sub>x</sub> films after irradiation. The data for unirradiated films was previously presented in [8]. Inset in figure 3(b) shows a typical  $G(T)$  function used to maintain the 'piecewise' continuity. Figure 3(c) shows a summary of the  $\mu$  values obtained from the slopes indicated with dotted oval in the figure 3(b). The results show that  $\mu$  values systematically decrease from  $\mu \approx 1.6$  to  $1.7$  for the optimal doped film [8, 33] to  $\approx 1$  for unirradiated  $x = 6.70$  before irradiation (see table 1).

The value for the latter after irradiation drops to  $\approx 0.66$ , maybe affected by the 2D to 3D crossover usually observed at  $T_c \approx 50$  K [15]. In the framework of the collective creep theory,  $\mu$  evolves from predictors for small (3/2) to large vortex bundles (7/9) as  $T_c$  reduces. Unlike clean systems such as single crystals, the vortex pinning in the films is produced by a combination of a low density of nanoparticles, island boundaries and random disorder [17, 25]. However, in analogy with columnar defects, if the number of vortices exceeds the number of nanoparticles, then the vortex dynamics be dominated by interstitial vortices trapped between the nanoparticles by the random disorder [26].

Our results show that disorder at the nanoscale produced either by changes in the oxygen stoichiometry or random disorder shifts  $T_c$  and  $J_c^{sf}$  in a similar manner. This correlation may be related to changes in the penetration depth  $\lambda$  [10, 34], and the reduction of the depairing critical current  $J_0 = cH_c/3\sqrt{6}\pi\lambda$  (with  $H_c(0) = \phi_0/2\sqrt{2}\lambda(0)\xi(0)$  the thermodynamic critical field,  $\xi(0)$  the coherence length and  $c$  the speed of light). Taking in consideration  $\xi(0) \approx 1.6$  nm and  $\lambda^7(0) \approx 120$  nm,  $\lambda^{6.95}(0) \approx 125$  nm  $\lambda^{6.88}(0) \approx 133$  nm (interpolated) and  $\lambda^{6.7}(0) \approx 190$  nm (interpolated) [33], we obtain  $J_c^{sf}/J_0 \approx 4\%–7\%$  for the different pristine samples. A direct correlation between  $\lambda$  and  $J_c^{sf}$  has been reported in type II superconductors [35]. Indeed, thin films with thickness less than  $\lambda$  display a  $J_c^{sf} \propto 1/\lambda^3$  dependence. Moreover,  $J_c^{sf} \propto 1/\lambda^2$  has been predicted for samples thicker than  $\lambda$  [35]. The changes in  $J_c^{sf}$  produced by oxygen stoichiometry are larger than those produced by irradiation [2, 8, 13]. Although irradiation with protons produces mainly random defects, the disorder should be more localized than that provided by oxygen vacancies [2]. In addition to the change in  $J_c^{sf}$ , we found a direct correlation between  $T_c$  and  $\mu$ . A strong suppression in  $J_c^{sf}$  is observed for  $x = 6.7$  after irradiation (see figure 2(b)), which may be related to the proximity to the 2D crossover and to changes in the oxygen order in the Cu chains [36]. The results should be interpreted considering the influence of the disorder at the nanoscale on the thermal fluctuations. Comparatively, for pinning produced by a high density of random nanoparticles (defined interfaces matrix-defect), the  $S$  values are smaller than those observed in irradiated samples [2, 6, 8, 9]. The difference has been related to the influence of the type of defects in the vortex bundle size [9]. Nevertheless, an aspect scarcely discussed in the literature is the role of nanoscale inhomogeneities on the mechanisms that determine the time decay of the persistent current densities. Unlike thin films with a high density of strong pinning centers and uniform  $T_c$ , in irradiated superconductors, local variations of the superfluid density may contribute to a more inhomogeneous distribution of persistent currents and faster relaxation rates.

#### 4. Conclusions

In summary, we performed a comparative study of the vortex dynamics in oxygen-deficient 1.3  $\mu\text{m}$  thick  $\text{GdBa}_2\text{Cu}_3\text{O}_x$  (GBCO) tapes with and without extrinsic point disorder added by proton irradiation. Unlike oxygen vacancies [13], extrinsic

defects added by proton irradiation produce a smoother magnetic field dependence of  $J_c$ . Despite this difference, we found a clear correlation between the  $T_c$ , the  $J_c^{sf}$  and the glassy exponent  $\mu$ . As  $T_c$  decreases from 93 K to  $\approx 55$  K,  $J_c^{sf}$  reduces from  $\approx 30$  MA  $\text{cm}^{-2}$  to  $\approx 1$  MA  $\text{cm}^{-2}$ , and  $\mu$  shifts from  $\approx 1.7$  to  $\approx 0.66$ . These values are close to the theoretical predictions for small and large bundles, respectively.

#### Acknowledgments

This work has been partially supported by Agencia Nacional de Promoción Científica y Tecnológica PICT 2015-2171. NH and JG are members of the Instituto de Nanociencia y Nanotecnología CNEA-CONICET (Argentina).

#### ORCID iDs

N Haberkorn  <https://orcid.org/0000-0002-5261-1642>

#### References

- [1] Kwok W-K, Welp U, Glatz A, Koshelev A E, Kihlstrom K J and Crabtree G W 2016 *Rep. Prog. Phys.* **79** 116501–39
- [2] Jia Y *et al* 2013 *Appl. Phys. Lett.* **103** 122601
- [3] Sadovskyy A *et al* 2016 *Adv. Mater.* **28** 4593–600
- [4] Mele P, Matsumoto K, Horide T, Ichinose A, Mukaida M, Yoshida Y, Horii S and Kita R 2008 *Supercond. Sci. Technol.* **21** 032002
- [5] Jha A K *et al* 2015 *Supercond. Sci. Technol.* **28** 114004
- [6] LeRoux M *et al* 2015 *Appl. Phys. Lett.* **107** 192601
- [7] Eisterer M 2018 *Supercond. Sci. Technol.* **31** 013001
- [8] Haberkorn N, Jeehoon K, Suárez S, Jae-Hun L and Moon S H 2015 *Supercond. Sci. Technol.* **28** 125007
- [9] Eley S, Leroux M, Rupich M W, Miller D J, Sheng H, Niraula P M, Kayani A, Welp U, Kwok W-K and Civale L 2017 *Supercond. Sci. Technol.* **30** 015010
- [10] Basov N *et al* 1994 *Phys. Rev. B* **49** 12165
- [11] Franz M, Kallin C, Berlinsky A J and Salkola M I 1997 *Phys. Rev. B* **56** 7882
- [12] Nachum B *et al* 1996 *Phys. Rev. Lett.* **27** 5421
- [13] Haberkorn N *et al* 2017 *Supercond. Sci. Technol.* **30** 095009
- [14] Chien T R, Datars W R, Veal B W, Paulikas A P, Kostic P, Chun G and Jiang Y 1994 *Physica C* **229** 273–9
- [15] Sefrioui Z, Arias D, Varela M, Villegas J E, López de la Torre M A, León C, Loos G D and Santamaría J 1999 *Phys. Rev. B* **60** 15423
- [16] Jae-Hun L, Hunju L, Jung-Woo L, Soon-Mi C, Sang-Im Y and Seung-Hyun M 2014 *Supercond. Sci. Technol.* **27** 044018
- [17] Haberkorn N *et al* 2017 *Physica C* **542** 6–11
- [18] Lee J H, Lee H, Lee J W, Choi S M, Yoo S I and Moon S H, 2014 *Supercond. Sci. Technol.* **27** 044018
- [19] Osquiguil E, Maenhoudt M, Wuyts B and Bruynseraede Y 1992 *Appl. Phys. Lett.* **60** 1627
- [20] Civale L, Marwick A D, McElfresh M W, Worthington T K, Malozemoff A P, Holtzberg F H, Thompson J R and Kirk M A 1990 *Phys. Rev. Lett.* **65** 1164
- [21] Kirk M A and Yan Y 1999 *Micron* **30** 507

- [22] Gyorgy E M, Van Dover R B, Jackson K A, Schneemeyer L F and Waszczak J V 1989 *Appl. Phys. Lett.* **55** 283
- [23] Yeshurun Y, Malozemoff A P and Shaulov A 1996 *Rev. Mod. Phys.* **68** 911
- [24] van der Beek C J *et al* 2002 *Phys. Rev. B* **66** 024526
- [25] Haberkorn N, Coulter Y, Condó A M, Granell P, Golmar F, Ha H S and Moon S H 2016 *Supercond. Sci. Technol.* **29** 075011
- [26] Blatter G, Feigelman M V, Geshkenbein V B, Larkin A I and Vinokur V M 1994 *Rev. Mod. Phys.* **66** 1125
- [27] Miura M *et al* 2011 *Phys. Rev. B* **83** 184519
- [28] Rupich Martin W *et al* 2016 *IEEE Trans. Appl. Supercond.* **26** 6601904
- [29] Maiorov B *et al* 2009 *Nat. Mater.* **8** 398–4004
- [30] Maley M P, Willis J O, Lessure H and McHenry M E 1990 *Phys. Rev. B* **42** 2639–42
- [31] Ossandon J G *et al* 1992 *Phys. Rev. B* **46** 3050–8
- [32] Thompson J R *et al* 1997 *Phys. Rev Lett.* **78** 3181–4
- [33] Polat O *et al* 2011 *Phys. Rev. B* **84** 025519
- [34] Sonier J E *et al* 2007 *Phys. Rev B* **76** 134518
- [35] Talantsev E F and Tallon J L , 2015 *Nat. Commun.* **6** 7820
- [36] Plakhty V, Stratilatov A, Yu C and Fedorov V 1992 *Solid State Commun.* **84** 639–44